Separation Science and Technology
Publication details, including instructions for authors and subscription information:
http://www.informaworld.com/smpp/title~content=t713708471

DEVELOPMENT AND MODELING OF A CONTINUOUS SIMULATED MOVING BED ION EXCLUSION PROCESS FOR THE SEPARATION OF ACID AND SUGAR

R. M. Springfield[a]; R. D. Hester[b]
[a] Mississippi Polymer Technologies, Bay Saint Louis, Mississippi, U.S.A. [b] University of Southern Mississippi, Hattiesburg, Mississippi, U.S.A.

To cite this Article Springfield, R. M. and Hester, R. D.(2001) 'DEVELOPMENT AND MODELING OF A CONTINUOUS SIMULATED MOVING BED ION EXCLUSION PROCESS FOR THE SEPARATION OF ACID AND SUGAR', Separation Science and Technology, 36: 5, 911 — 930

To link to this Article: DOI: 10.1081/SS-100103628

URL: http://dx.doi.org/10.1081/SS-100103628

SEPARATION SCIENCE AND TECHNOLOGY, 36(5&6), 911–930 (2001)

DEVELOPMENT AND MODELING OF A CONTINUOUS SIMULATED MOVING BED ION EXCLUSION PROCESS FOR THE SEPARATION OF ACID AND SUGAR

R. M. Springfield[1] **and R. D. Hester**[2]

[1]Mississippi Polymer Technologies, 13233 Webre Road,
Bay Saint Louis, Mississippi 39520
[2]University of Southern Mississippi, Box 10076,
Hattiesburg, Mississippi 39406

ABSTRACT

The emission of large quantities of the greenhouse gas carbon dioxide into the atmosphere, as well as our increasing dependence on foreign oil supplies and the need to stimulate the lagging farm economy, has prompted research in the production of renewable liquid fuels from lignocellulosic materials. Acid hydrolysis of the cellulosic fraction of these materials into sugars that can be fermented to ethanol is one option. In support of this approach, a simulated moving bed ion exclusion chromatography system was constructed for the continuous separation of the product sugars from the acid used to effect hydrolysis. A numerical simulation model of the process is presented here. Our system consisted of 4 zones of 18 resin-packed columns, each approximately 820 mL in size, arrayed about a central manifold system using solenoid valves to control fluid flow. The model is based upon experimental data from the system arrayed with 9 doubled and 18 single columns. The numerical simulation model was used in conjunction with statistical experimental design techniques to probe the optimum op-

erating conditions: the selection of the simulated flow rate, the number of columns needed in each zone and the appropriate number of columns in the system as a whole. A development facility more than 10-times the current system size is being pursued.

INTRODUCTION

This paper presents part of the work to develop a commercializable process for the conversion of lignocellulosic materials to fuel-grade ethanol. Candidate lignocellulosic materials include agricultural waste, crops such as grasses with high cellulose content, under-utilized and short rotation forest products, and municipal solid waste. The process utilizes sulfuric acid to hydrolyze cellulose into simple sugars. After removal of residual lignin, the resulting acid/sugar mixture or hydrolyzate is separated allowing reuse of the acid and fermentation of the sugars to produce fuel-grade ethanol. Among the many benefits arising from the efficient conversion of lignocellulosic resources to fuels are

- A substantial reduction in the emission of carbon dioxide from vehicle exhaust emissions with an overall improvement in air quality.
- Recovery and utilization of waste materials.
- Added value for agricultural and forestry crops.

This paper describes the numerical simulation of the acid recovery system: a continuous simulated moving bed (SMB) ion exclusion chromatography system used to separate the hydrolyzate into an acid-rich stream and a sugar-rich stream. The simulation development is part of a scale-up plan for commercialization. This SMB system is a laboratory scale continuous separation process consisting of 18 resin-packed columns connected by flow control valves. The following discussion reviews the process before addressing the model and results.

Process Overview

As previously reported (1) and shown in Figure 1, the major systems in this process for the conversion of lignocellulosic materials to ethanol and lignin:

1. Lignocellulosic solids feed and acid impregnation
2. Hemicellulose and cellulose hydrolysis to sugars
3. Lignin separation
4. Acid recovery and sugar separation
5. Acid concentrated
6. Sugar concentrated
7. Fermentation of the pentose and hexose sugars to ethanol

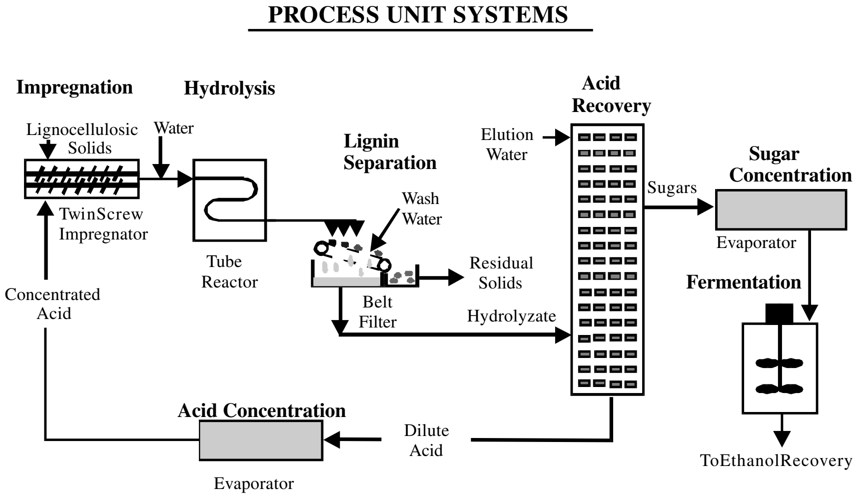

Figure 1. Process schematic.

The impregnation system continuously exposes the lignocellulosics to concentrated sulfuric acid under high-shear conditions. The acid serves as a catalyst in the continuous hydrolysis reactor. High temperature hydrolysis of the acid impregnated cellulosic materials produces an aqueous sugar/acid solution called hydrolyzate. The Lignin Separation system removes the residual solids in the hydrolyzate above 5μm in size using a belt filter and membrane filters. The hydrolyzate, an aqueous solution of acid (~12-wt. %) and sugars (~5-wt. %), is then pumped into the recovery system. The Acid Recovery system uses continuous ion exclusion to separate the hydrolyzate into acid-rich and sugar-rich aqueous streams. The acid-rich stream is concentrated to 70-wt. %, by evaporation and then recycled to the Impregnation system. The sugar-rich stream is concentrated by evaporation to 9.5-wt. % sugar and fermented.

SEPARATION SYSTEM DESIGN

The separation system used for this research is a classical simulated moving bed design using Ion Exclusion Chromatography (IEC) to separate the solute molecules. After outlining the principles involved in IEC and discussing the SMB design used for this study, the model will be addressed.

Ion Exclusion

Wheaton and Bauman first noted IEC in 1953 (2). The foundational principle of this technique is that the concentration of an electrolyte in a polar solvent is lower within the pores of a microporous ion exclusion resin than in the interstitial (hereafter referred to as macropore) volume. The resin used in these early experiments was a strong cationic exchange resin (sulfonated poly(styrene-co-divinylbenzene)) in the hydrogen form and is similar to the resins used for this project. Wheaton and Bauman noted that the resin had to be of the same ionic charge as the ionic portion of the materials being separated (2). Figure 2 shows a schematic representation of the resin bed structure highlighting the micropores and macropores. Separation results from differences in the path the solute molecules travel, which depends upon the size and ionic nature of the solute.

The mean path length for a charged solute molecule through an ionic chromatographic system is greatly influenced by coulombic repulsive forces. Ionic separation of differing solute molecules is achieved if they have sufficiently different ionic character. Conditions that contribute to good separation between ionic and non-ionic molecules include low ionic concentrations in the feed stream, small feed-to-solvent volume ratios, low feed rates, and elevated temperatures (3, 4).

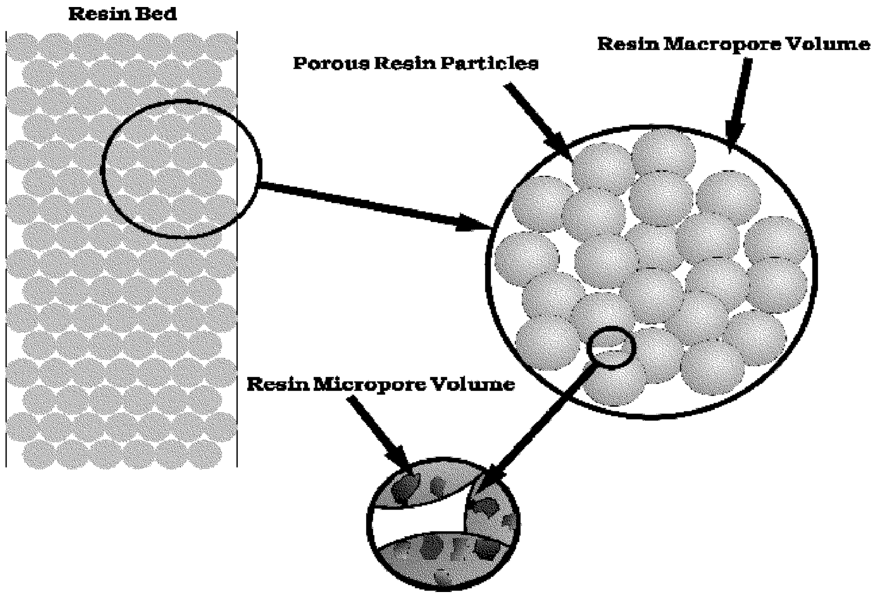

Figure 2. Resin bed schematic.

Simpson and Wheaton have shown that the most important descriptive parameter for separations using IEC is the difference in the distribution coefficient (5). Distribution coefficients describe the ratio of the concentrations of solute molecules in the micro- and macropores of the chromatography column. One influence on the distribution coefficient in an IEC system is resin swelling or shrinking in the column. A polar solvent, used as the mobile phase in the chromatography system, typically swells the resin. Resin swelling is a response to an imbalance between osmotic pressure and the retractive forces acting on the polymeric chains of the resin. The swelling yields resin volume changes that reflect the new equilibrium of these forces. For example, an increase in the local ion concentration would reduce the electrostatic repulsive forces and result in micropore shrinkage. On the other hand, an increase in temperature allows the polymer to relax reducing the retractive forces and increasing the micropore volume.

Ionic species are excluded from the micropores as explained by the Donnan exclusion principle, which states that the electric potential in the resin must remain balanced (6). Therefore, since the sulfonate group is physically attached to the polymer composing the resin, other ions are predominately excluded from the resin because their presence within the resin would disrupt the electric potential balance. The ionic species is therefore excluded from the microporous resin interior volume because the resin walls repel the ionic species with like charge. In contrast, the non-ionic species have free passage into the micropore volume because they have no ionic charge. Because of this ionic exclusion, the interior volume of the resin becomes saturated with non-ionic species when it is exposed to the feed. Note, however, that while the ionic species is excluded from entering the resin, it also is changing the balance of forces on the particle and causing shrinkage of the resin particle. This shrinkage will effect the ability of the non-ionic species to move into and out of the resin particle. In addition, Saska has shown that the presence of sugar can change the diameter of the resin particle (7). This effect is assessed as being the result of the change in the degree of hydration of the resin particle. These changes in particle diameter, in addition to impacting the separation efficiency, are also shown to impact the kinetics of the mass distribution process. Ching has shown that in high concentration regimes the sugar absorption isotherm is non-linear (8). This, according to Saska, is in part attributable to the resin particle diameter changing with a change in species concentration (7). In the case of an acid/sugar separation both the acid and the sugar can affect the hydration of the resin particle and thus the separation performance.

Simulated Moving Bed Systems

The idea of simulated moving beds dates from the 1840's, according to Wankat (9), and has been used in many separation applications, including petrochemicals and agriculture (9, 10). For our purposes we will focus on the application of Simulated Moving-Bed (SMB) systems to the Ion Exclusion Chromatography (IEC), the application of interest. SMB IEC systems are composed of a series of beds packed with a microporous ion exchange resin. Simulated movement of the resin bed and the flow of fluid through the interstitial bed volume carry the non-ionic species away from the ionic species, which are principally located within the interstitial volume of the beds. The ionic species is removed from the SMB IEC system in an ionic species-rich stream. The non-ionic species are later forced out of the bed and removed from the SMB IEC system by a continuous flow of fresh elution fluid, in our case water, countercurrent to the resin movement. The resin, now free of non-ionic species, is recycled to be again exposed to the feed and thus continuously repeat the separation process.

A SMB IEC system for acid-sugar separation similar to that described by Hartfield (3) is shown in Figures 3 and 4. Figure 3 shows the conceptual arrangement of the different zones of the system and illustrates the countercurrent flow of resin and fluid in an SMB system. Figure 4 illustrates how sequencing the column beds simulates resin flow by following column three through a complete cycle. At specific times, flow valves may be set so that any column would correspond to the top of Zone I, in Figure 3. For example, in Time III of Figure 4, Column 3 is the top of Zone I.

Acid/Sugar Separation SMB IEC System Configuration

Specifying the columns having the acid/sugar feed input stream, water input stream, sugar-rich takeoff stream, and acid-rich takeoff stream configures fluid

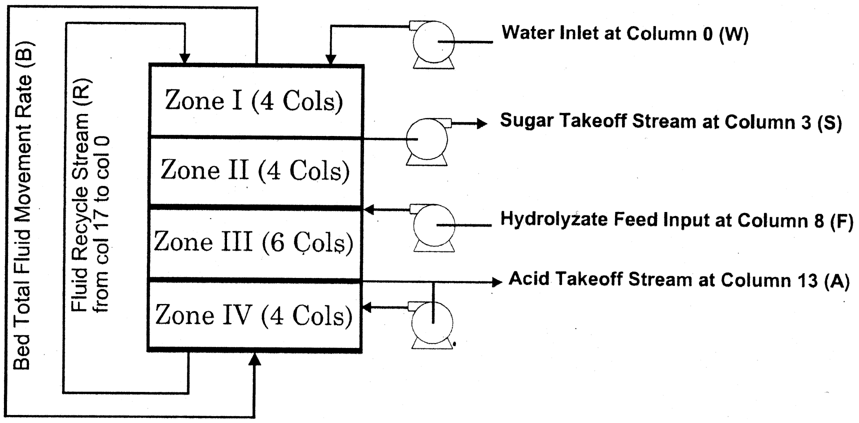

Figure 3. Idealized SMB system.

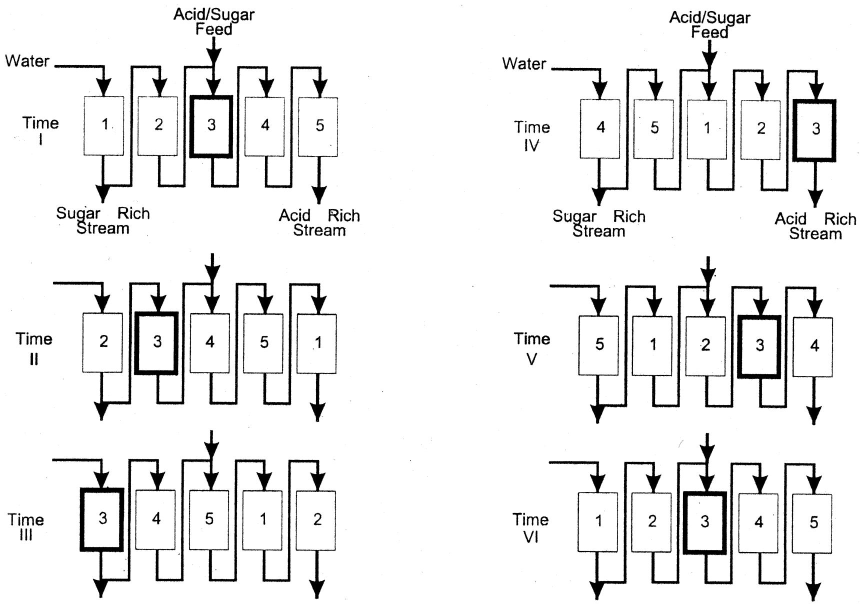

Figure 4. SMB cycle.

movements throughout the system. In addition, the input and output columns for internal system recycle must be defined. Also, the rate of bed fluid movement on a per column basis must be established by specifying the valve shift times, that is the time allotted to each system configuration as determined by the fluid-flow control valves. The fluid movement rate is given by dividing the total column fluid by the shift time. All these parameters are inputs to the model.

Although all columns are at the same elevation, for discussion purposes, we can consider the system to be stacked vertically with a continuous flow of fluid from top to bottom. The ``top column'' of the SMB IEC system is always considered the column having the elution water inlet stream as shown in Figure 3. The direction of column bed movement is always from the bottom of the system to the top of the system, thus the resin movement can be considered to go up the SMB IEC system.

SMB systems have been used with both three and four zones; however, the four-zone system offers a more economical use of elution fluid (11). The most familiar four-zone system is UOP's Sorbex family of separation processes (12, 13). As shown in Figure 3, Zone I is from the water inlet through the sugar takeoff stream. Zone II is from the inlet below the sugar takeoff stream through the column preceding the acid/sugar feed stream inlet column. Zone III is from the acid/sugar feed stream inlet through the acid takeoff stream. Zone IV consists of all the columns remaining in the system from the inlet below the acid takeoff stream to the last column. The process is analogous to a distillation process in which Zones IV and I function as condenser and reboiler as noted by Ruthven and Ching (11).

Each zone of columns performs a specific function. The columns of Zone I function to purge sugar from the resin micropore volume and provide for its removal via the sugar takeoff stream. Zone II columns separate the acid from the sugar in the micropores. Zone III columns allow the resin micropore fluid to saturate with the sugar being introduced from the acid/sugar feed stream. In Zone III, sugar in the micropore fluid is carried up by the simulated upward flow of bed resin. Zone IV columns are labeled as a "solvent saver'' zone by UOP writers, while Hotier recommends considering this as simply a buffer zone (13, 14). Regardless, due to the Zone flow rate requirements for correct system operation, only solvent passes from the last column in the system to the top and any acid entering Zone IV is carried upward for removal from the system (11).

Ruthven and Ching have compiled an excellent review paper detailing countercurrent and simulated countercurrent absorption processes (11). Ruthven and Ching divide modeling approaches based upon representation of the system, on the bed elements, and on whether the treatment is equilibrium theory based or based on a linear driving force model using a rate equation to account for mass transfer resistance. System representations deal with the distinction between a true continuous countercurrent depiction and a direct simulation of port switching. The bed elements can be resolved either by a plug flow or axial-dispersed plug flow model or as equilibrium mixing cells. We have chosen to make use of numerical simulation of direct port switching using mixing cells. This method allows generation of the transient profiles as the system approaches equilibrium as well as the final equilibrium condition; however, it is more computationally intensive as noted by Ruthven and Ching. Nanguneri noted that the local acid concentration affects the separation and Ruthven and Ching noted that nonlinear and/or coupled equilibria require a special approach to modeling (4, 11). We find that a model similar to what is needed in this study is described by Ching (15). The following section will describe the theoretical basis of our model.

CONTINUOUS ION EXCLUSION SEPARATION MODEL

To model our system, we have chosen an equilibrium mixing cell numerical simulation of the system. This approach allows for complete simulation of the process without appeal to complex mathematical descriptions of the mass transfer and fluid flow. Mass transfer resistance and dispersive effects are accounted for by the size assigned to the equilibrium cells in the model. At small step sizes this approximation should not introduce excessive error (16).

In the mixing cell approach, the system is divided into equilibrium units called theoretical plates, or more accurately, into bed lengths corresponding to the height equivalent of a theoretical plate (HETP). In general, HETP is a function of mass flow rate, diameter of the packing material particles, degree of cross-linking in the particles (controlled by the content of divinyl benzene in the resin formulation), loading of species to be separated on the packed bed, etc. In our model, the bed is actually meshed in smaller units to increase the numerical stability of the solution. These smaller units are handled in small increments and the resulting mass distribution is then averaged to reflect equilibrium considerations.

Ching notes that the system species profiles computed by a model are much more sensitive to the equilibrium relationships than the value assumed for HETP, and thus it is difficult to assess the assumption of constant HETP within the system (15). In our model we change the HETP based upon local flow rate and concentrations. The magnitude of these changes was fitted to the experimental data during model development.

Because the particle diameter is a function of local species concentration, the particle diameter is considered indirectly in the HETP value. As was described in the introduction, the dominant change in particle diameter is driven by the acid concentration effect on the osmotic pressure in the particles themselves. We have elected to reflect the fact that the acid has a strong affect upon the sugar and the sugar a minimal impact upon the acid by using the following equations to define the distribution coefficient for each species, K_{Acid} and K_{Sugar}. The distribution coeffiecient for the acid is given by,

$$K_{Acid} = K0_{Acid} - A_{Acid} * \text{PlateFlowRate}$$

while the sugar is given by

$$K_{Sugar} = K0_{Sugar} - A_{Sugar} * \text{PlateFlowRate} + B * C_{Acid}.$$

These functions account for the effect of flow rate on the kinetics of separation. The sorption process is kinetically constrained in part due to the geometry of the resin. The K0's are the distribution coefficients measured at equilibrium conditions. A and B are empirically derived constants and C_{Acid} is the local acid concentration

According to Saska, Monosphere 99 resin has a volume weighted mean pore diameter of approximately 10 Å; that is, half the resin pores are larger than 10 Å. Saska then concludes that a large fraction of the pores are of about the same diameter as the hydrated sugar molecule (sucrose is approximately 5 to 7 Å) and penetration into the resin pores requires displacement of hydration layers (7). This geometric constraint is made evident in the flow rate term by the effective distribution coefficient used in our model where the time element of the diffusion into and out of the resin is affected by the exposure time or the flow rate.

Other model parameters include the bed geometry terms, the feed composition, and the cycle definition. The geometry terms include length and diameter of a single bed, as well as the number of beds in the system and the number of mixing cells per bed. The feed composition includes both the acid and sugar concentrations in the feed stream. The cycle definition includes the valve switching time and the number of beds in each of the four zones.

COMPARISON OF THE MODEL AND EXPERIMENTAL DATA

Previously (1), we reported the experimental results obtained from running our SMB-IEC system in three different configurations. The following will discuss the results obtained by fitting the model to Process I, an 18-column configuration, and then looking at the 9-column configuration (Process II) and conclude with some optimization studies.

Process I

Process I was chosen as the benchmark for the model (all the model output in this section of the document is from the same model output). As can be seen in Figure 5 below, the model fit is not exact. However, after considering the estimated experimental error (shown as error bars) the model fit is reasonable. The error arises from both fluid sample collection difficulties and inherent error in analyzing the data. Column 9 is the feed column and thus we are measuring both the system concentration and the feed contribution when sampling. This adds to uncertainty for the columns 8 through 10. Zone III, found in columns 9 through 14, has a fair sugar fit to the concentration data and slightly over predicts the acid concentration. Project constraints precluded more accurate data collection. Thus, the model fit is considered adequate at this level of data uncertainty. We will now consider the model fit and what is provided from the model output.

An important comparison for the model with experimental data is the variation of the output stream concentrations during each time increment. This variance was noted, but was not carefully characterized due to lack of project resources. This variance has been noted by other researchers such as Hotier in his work with the separation of glucose and fructose (14). Figures 6 and 7 show our model output for this effect. As can be seen in Figure 6, the SMB-IEC sugar output stream, from a concentration of 7.8% to 12.7%. A 10% sugar concentration is required for fermentation. Figure 6 indicates that a 10% sugar concentration may

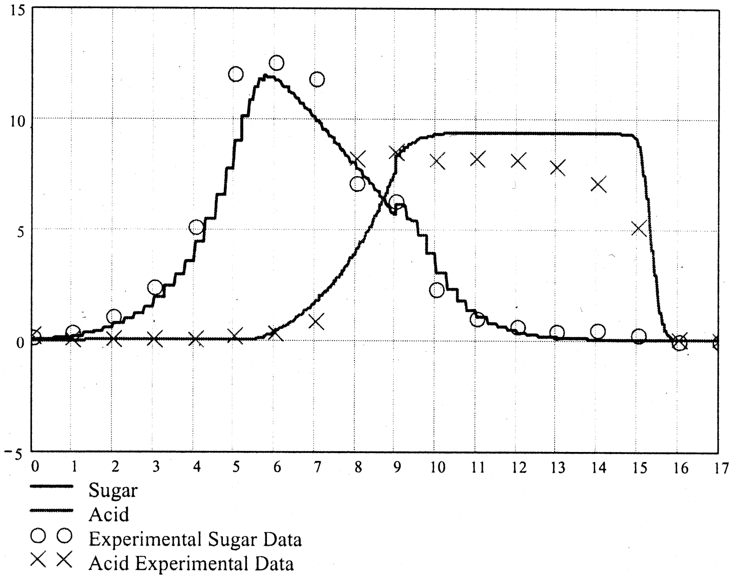

Figure 5. Process I and model output.

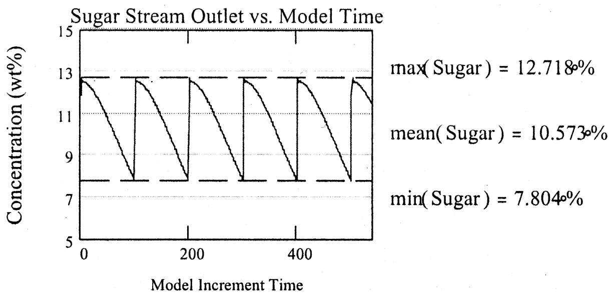

Figure 6. Sugar outlet stream concentration.

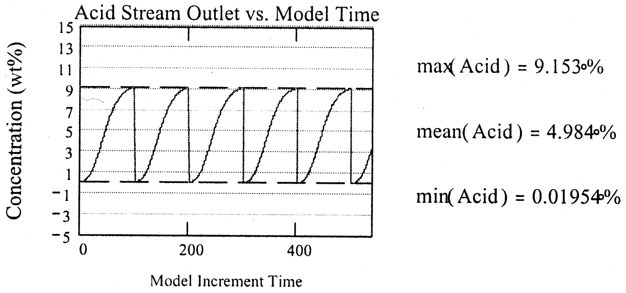

Figure 7. Acid outlet stream concentration.

Marcel Dekker, Inc.
270 Madison Avenue, New York, New York 10016

be achievable directly from the recovery section; thus, eliminating an evaporation step to concentrate the sugar within this stream. Eliminating the requirement for an evaporator will save capital and energy in a commercial plant design. Hotier's work demonstrates a similar occurrence with the concentration dropping as the cycle progresses (14). Concentration decreasing in the extract stream is related to dilution by the elution fluid. This is the inverse of what happens in the acid stream as may be seen in Figure 7. While the acid stream fluctuates also, the concentration values for the acid stream vary from 9.5% (nearly equal to the feed concentration) to 0.0%, a much greater variance. This variance opens the potential for splitting the acid stream into a high acid concentration-fraction and a low acid concentration-fraction stream. There are several possible uses in the process for the dilute or low acid concentration-fraction stream, including using the fluid for part of the solids washing step or as dilution fluid for the impregnated material coming out of the extruder. The higher acid concentration stream will require less energy for evaporation to the impregnation system acid-feed concentration of 70%.

Reflection on the function of the system makes the source of these variations evident. Taking the acid stream as an example, it can be seen that immediately following an increment of the column duties (that is an incrementing of the open valves across the system) the column which now exits to the acid removal stream was previously in the "solvent saver zone" and initially has effectively no acid at its outlet. As time passes, the acid progresses down the system and the concentration in the outlet stream increases, reaching approximately the feed concentration when at the end of the cycle the valves once again are repositioned. Thereafter the process repeats. Thus, one may conclude from the data and the literature confirmation that our model predicts correctly, within the limits of the data accuracy, the output stream concentration cycling.

A third point of consideration is available to provide insight into the model and help identify any potential problems. This involves assessing the actual parameters which influence the separation, predominately the species distribution coefficients. Figure 8 shows these parameters as well as the theoretical plate heights and the flow rate for each zone. It can be seen from Figure 8 that the sugar distribution coefficient is constant in the first zone where a high fluid flow rate is washing the sugar from the resin bed and driving it from the system. In the second zone, the flow rate is lower and the sugar distribution coefficient is responding to the presence of the acid (which affects transport of the sugar molecules into the resin particles) and the decrease in the flow rate. At the beginning of the third zone there is a discontinuity in the sugar distribution coefficient, which is associated with the feed inlet. Following this, the sugar distribution coefficient stabilizes as the flow rate and acid concentration are effectively constant in Zone III. Finally, in zone four there is a discontinuity at the transition from zone three where the acid concentration and the flow rate experience substantial change. Thereafter, the dis-

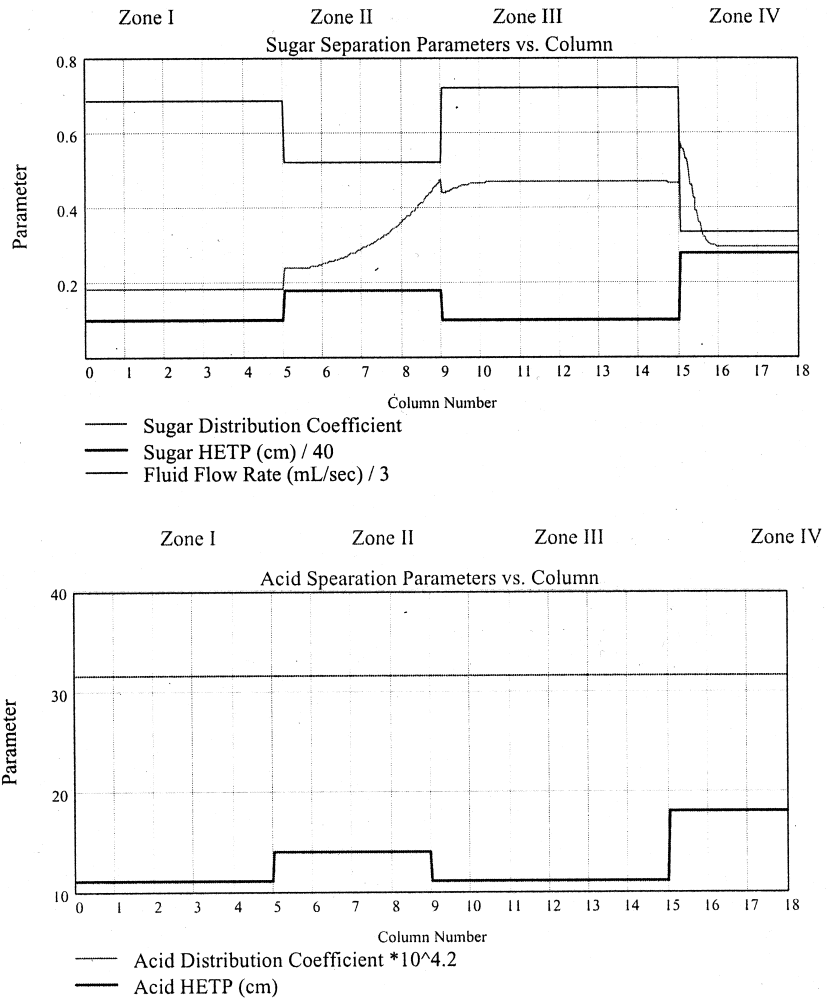

Figure 8. HETP and Kd for sugar and acid.

tribution coefficient again stabilizes to a constant value in Zone IV. The sugar distribution coefficient is higher in Zone IV than Zone I. This is expected because the flow rate is lower in Zone IV relative to Zone I. The only unanticipated result for the sugar distribution coefficient is the large magnitude of its value in Zone III. Therefore, the sugar distribution coefficient, which is in actuality a function of many influences, is more strongly affected by the presence of the acid than anticipated. The Sugar HETP follows a pattern consistent with the flow rate; and, in as much as we have modeled most of the variables that influence the sugar separation into the distribution coefficient, this parameter is less critical in affecting model separation performance.

The acid distribution coefficient, also shown in Figure 8, was found to best fit the experimental data as a constant. This is consistent with what one would expect for the ionic species in an ion exclusion process; that is, the acid has very little penetration into the resin. The acid HETP is also shown in Figure 8 for reference and again tracks with what one would anticipate.

A final point of consideration for the model is shown in Figure 9. Here we see that the model rapidly approaches a steady state condition and stabilizes. Experimentally it was found that approximately 12 cycles were required before steady state was established. This discrepancy is not everly distressing as the model assumes perfect control of the flow and does not have to deal with the induced error from sampling. Therefore the results from the model are seen as consistent with what one should expect from a system which operated with inline real time sampling devices. Note also that in this case the model is predicting an excellent separation of better than 99% on both streams. In conclusion, the model

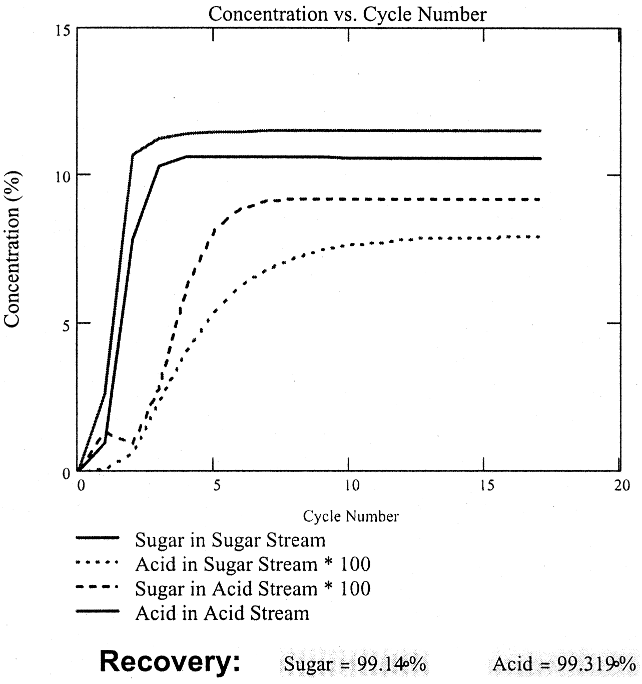

Figure 9. Model approach to steady state.

performance when compared against the base case data of Process I is considered acceptable. In the following sections we will address the tests performed to address the feasibility of reducing the number of columns (Process run II) and also include a look into the optimization of an idealized SMB-IEC system.

Process II

In the case of Process I, we were fitting the model to the experimental data by adjusting thirteen parameters, which address the physical character of the separation. For Process II we must adjust ten parameters, which control the system configuration, including the number of columns in each zone, the number of subincrements for each column, the number of theoretical plates allowed per zone, and the physical length of the column. And finally we have six parameters, which allow us to adjust the fit, that is the flow rates on the inlet streams and the concentrations of the species in the feed stream. Thus, to obtain the fit shown in Figure 10, we only adjusted the flow rates and concentrations of the inlet streams. For Process II, the model predicted acid profile agrees well with the experimental data, with the exception of column 14. For column 14, it appears that the titration analysis for acid concentration must have been in error since it is not reasonable to expect the acid concentration to suddenly decrease at that location. All the other

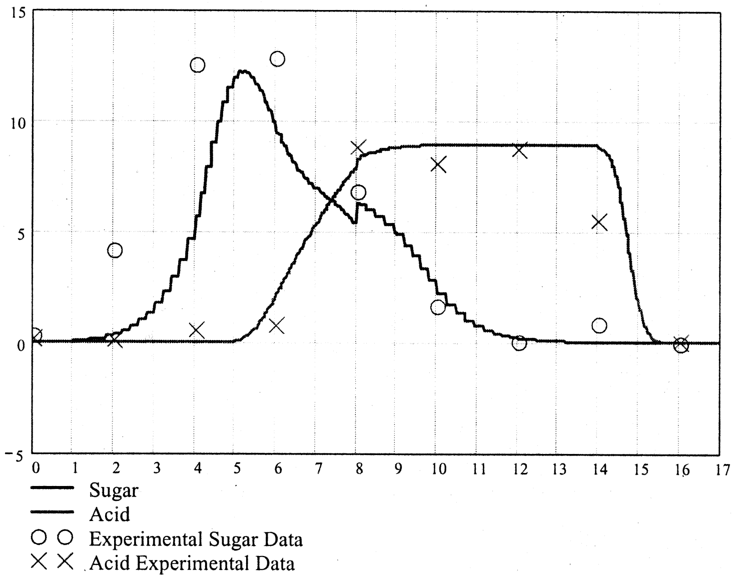

Figure 10. Process II and model output.

differences between data and model prediction seem to be within the error envelope for the data measurements that is produced by the time lag in actually making a data measurement versus the instantaneous value predicted by the model. The sugar curve from the model is less pleasing for the points at columns 2, 4, and 6. The point at column 6 is reasonably assumed to be due to a titration error. And, given the difficulty in controlling the flow rate in the experimental system with only nine control columns, the points at 2 and 4 may be considered accepted. Thus, we again have a fair model match with the experimental data.

OPTIMIZATION STUDIES

Since the model does an acceptable job of fitting Processes I and II, a potential use for the model is determining the optimum number of columns, or rather resin volume, per zone. In this case we used the Stat-ease experimental design software as used for the experimental design for Process II (17). This study uses a simplex design to probe the question regarding the optimum number of columns per zone. To facilitate the experimental design, we have used 10 columns rather than the 9 from Process II. The simplex design allowed the numbers of columns in a zone to vary from 1 to 7 in each of the four zones. Following running the model configured for each of the experimental design conditions, we used the numerical optimization routine in the Design-Expert software to find candidate optimum points. The best of the candidate points produced the results shown in Figure 11. This best configuration was defined with 4 columns in Zone 1, 2 columns in Zone II, 3 columns in Zone III, and 1 column in Zone IV. As seen from Figure 11, the model has predicted excellent separation. Also, note that we have used a higher acid feed concentration based upon expectations for a pilot plant. The pilot plant design has been documented elsewhere (18). Note that the mean acid concentration is much improved in comparison to Process II in this configuration.

It is also possible to use the model to study the effects of shift time upon the separation. Figure 12 shows the impact of shift time upon our optimum number and arrangement of columns. For this study we have used shift times based upon the shift time used in Process II, 6.2 minutes. Our test involved five conditions: 5.0, 5.6, 6.2, 6.8, and 7.4 minutes. Both species respond as one would anticipate; for example, the sugar recovery passes a maximum and falls as the shift time passes the base shift time of 6.2 minutes. The acid will fall at higher shift times. This SMB-IEC system uses 10 columns rather than the 9 of Process II, which it is based upon. Since we have added one column it is not unreasonable to find that the optimum shift time is slightly greater than was needed for 9 columns. The addition of bed length (or rather volume) to the SMB-IEC system causes this increase. Fluid counter-current flow is a function of the shift time and the bed length. It is necessary to balance the fluid flow within the system and the counter-current

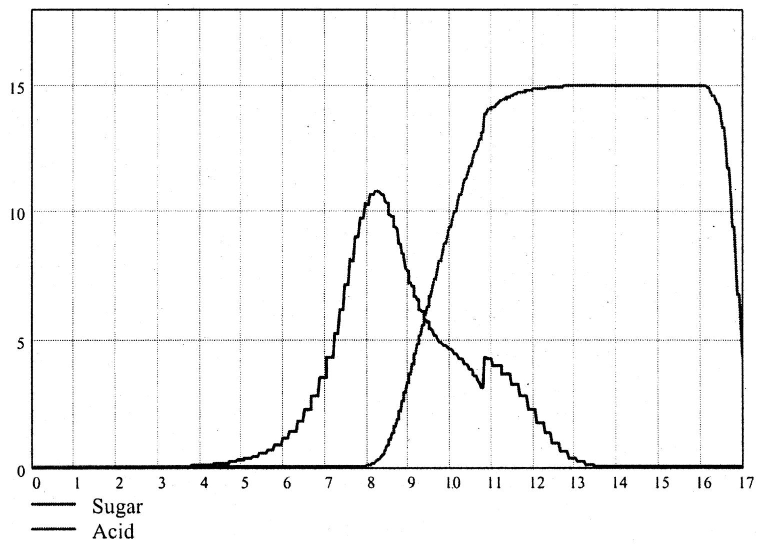

Figure 11. Optimized column array model output.

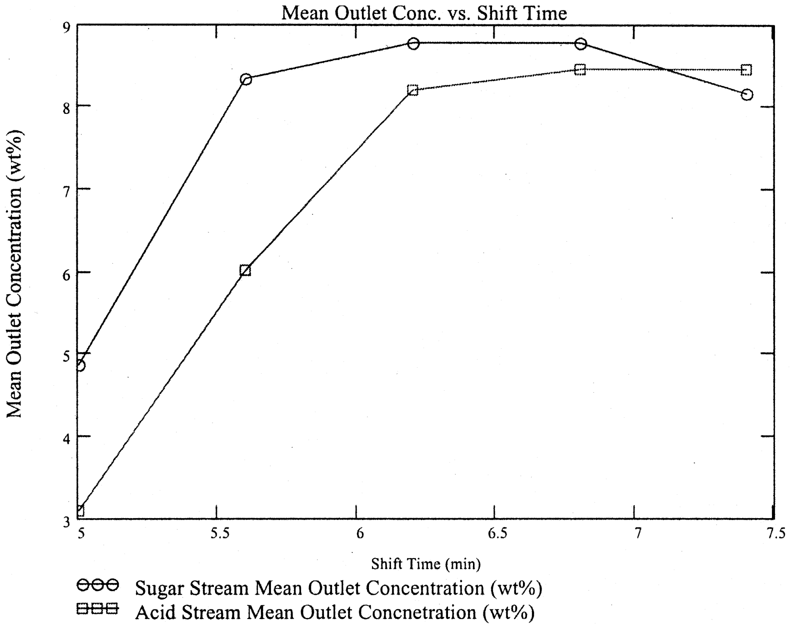

Figure 12. Shift time optimization results.

flow. Thus, in order to maximize the separation, increasing the bed length would be expected to necessitate an increase in the shift time. This allows the fluid to propagate through the system to the same degree, as was the case when the system has one less column of resin.

A final application of the simulation to the process involved developing contour plots depicting the effect of changing the water and or recycle flow rate. The simulation was configured using a 10-column array similar to that used in the previous optimization studies with the zones consisting of 4, 2, 3, and 1 column respectively. In this case, elution water flow rate and the sum of the elution water and the recycle fluid were selected as the test variables. Valve switching time is determined using a function (2929290/(water flow rate + recycle flow rate) = shift time in minutes) that is unique to the system we have modeled.

Analysis of the sugar in the acid-rich stream, shown in Figure 13, indicates higher water flow rates will reduce the concentration of sugar in the acid-rich stream. This is at the expense of process economics as more water usage results in greater energy for reconcentration of the acid-rich stream. The contour plot will allow an operator some guidance, given a maximum allowable sugar concentration in the acid-rich stream, to select proper water and recycle feed rates. A companion figure showing the acid in the sugar-rich stream is shown in Figure 14. It is apparent that the recycle flow pushes the acid away from the sugar stream as it increases within the bounds of the simulation flow rates.

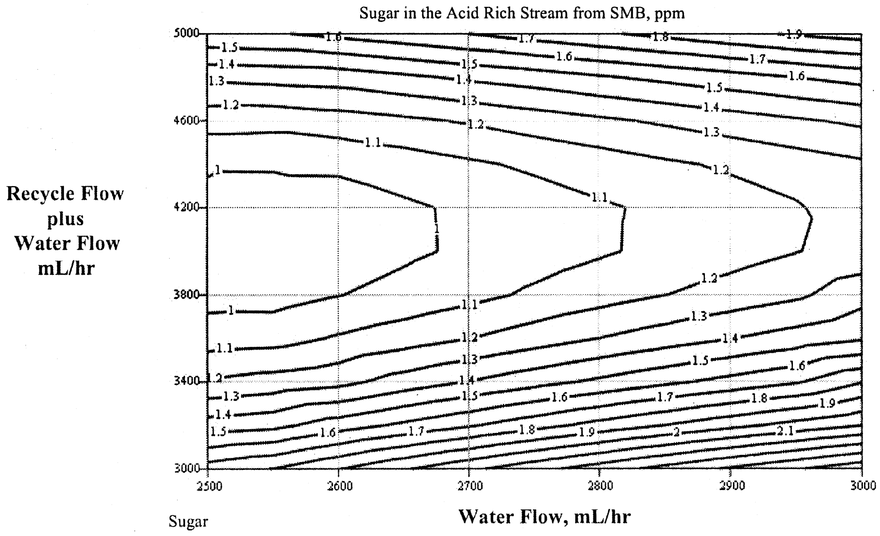

Figure 13. Predicted sugar concentration in acid rich stream.

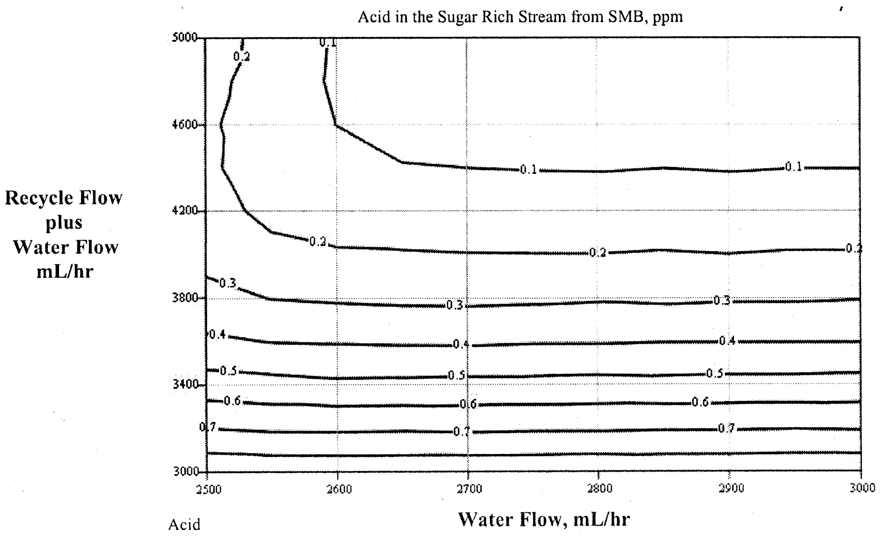

Figure 14. Predicted acid concentration in sugar rich stream.

CONCLUSIONS

A numerical model for the SMB-IEC system has been developed and successfully tested against experimental data. This model provides an adequate fit to the experimental data and satisfies the intent to fit the SMB-IEC system separation process using numerical modeling. The model functions to provide insight into the system operation. SMB-IEC system simulations have been used as a tool for understanding system separation performance and to predict optimum operating conditions and system configurations. Online detectors in plant systems will allow the model to be used to improve process performance to provide process control.

ACKNOWLEDGMENTS

Funding was provided by APACE Research Ltd., the Energy Research and Development Corporation of Australia, and the Tennessee Valley Authority. Portions of this work were performed for APACE and the ERDC under project number 2537. The authors also wish to thank Klenzoid Equipment Company's Jack Tobe for assistance in procuring resins.

REFERENCES

1. R. M. Springfield, R. D. Hester, "TENTH SYMPOSIUM ON SEPARATION SCIENCE AND TECHNOLOGY FOR ENERGY APPLICATIONS - Continuous Ion-Exclusion Chromatography System for Acid/Sugar Separation", Separation Science and Technology, **34** (6), 1217 (1999)
2. R. M. Wheaton, and W. C. Bauman, Ind. Eng. Chem., **45,** 228-233 (1953).
3. S. W. Hartfield, *Design and Analysis of an Ion Exclusion Chromatography Miniplant for the Separation and Acid and Sugar*. Masters Thesis, USM (1993).
4. S. R. Nanguneri, *Design, Development, and Analysis of a Preparative Scale Ion Exclusion Chromatography System*, Ph.D. Dissertation USM (1991).
5. D. W. Simpson, and R. M. Wheaton, Chem. Eng. Prog., **50,** 45-49 (1954).
6. F. Heffelrich, *Ion Exchange,* McGraw-Hill, NY (1954) pages 134-136, 431-433.
7. M. Saska, S. J. Clarke, M. D. Wu, K. Iqbal, J. Chrom **590** 147-151 (1992).
8. C. B. Ching, C. Ho, K. Hidajat, D. M. Ruthven, Chem. Engng. Sci. **42** (11) 2546-2555 (1987).
9. P. C. Wankat, *Large Scale Adsorption and Chromatography*, Vol 2, CRC Press, Boca Raton, Florida (1986)
10. K. Iqbal, Recovery of Sugars from Cane Molasses by Continuous Simulated Moving Bed Ion-Exclusion Chromatography, Ph.D. Dissertation, Louisiana State University, Baton Rouge, LA (1992).
11. D. M. Ruthven, and C. B. Ching, Chem. Engng. Sci., ***44,*** 1011 (1989)
12. D. B. Broughton, Continuous sorption process employing fixed bed of sorbent and moving inlets and outlets, U.S. Patent 2,985,589 (1961).
13. J. A. Johnson, G. F. Maher, and H. W. Dandekar, Industrial Applications of the Sorbex Process, AIChE 1993 Annual Meeting, St. Louis, MO (1993)
14. G. Hotier, AIChE J. ***42,*** 154 (1996)
15. C. B. Ching, C. Ho, D. M. Ruthven, Chem Engng Sci **43**(3) 703-711 (1988)
16. Z. Ma, N.-H. L. Wang, AIChE J. **43** (10) 2488-2508 (1997)
17. Design-Expert 5.0.9, Stat-Ease Corporation, Minneapolis, MN (1996)
18. R. D. Hester, R. M. Springfield, and G. E. Farina ″A Research, Development and Demonstration Plant for the Conversion of Lignocellulosic Materials into Ethanol and Lignin - Design and Cost Analysis for the Unit Systems of Impregnation, Hydrolysis, and Acid Recovery,″ Final Report, Project # TV96851V, Tennessee Valley Authority, Knoxville, TN., Oct., 1997.

Downloaded At: 10:48 25 January 2011

Request Permission or Order Reprints Instantly!

Interested in copying and sharing this article? In most cases, U.S. Copyright Law requires that you get permission from the article's rightsholder before using copyrighted content.

All information and materials found in this article, including but not limited to text, trademarks, patents, logos, graphics and images (the "Materials"), are the copyrighted works and other forms of intellectual property of Marcel Dekker, Inc., or its licensors. All rights not expressly granted are reserved.

Get permission to lawfully reproduce and distribute the Materials or order reprints quickly and painlessly. Simply click on the "Request Permission/Reprints Here" link below and follow the instructions. Visit the U.S. Copyright Office for information on Fair Use limitations of U.S. copyright law. Please refer to The Association of American Publishers' (AAP) website for guidelines on Fair Use in the Classroom.

The Materials are for your personal use only and cannot be reformatted, reposted, resold or distributed by electronic means or otherwise without permission from Marcel Dekker, Inc. Marcel Dekker, Inc. grants you the limited right to display the Materials only on your personal computer or personal wireless device, and to copy and download single copies of such Materials provided that any copyright, trademark or other notice appearing on such Materials is also retained by, displayed, copied or downloaded as part of the Materials and is not removed or obscured, and provided you do not edit, modify, alter or enhance the Materials. Please refer to our Website User Agreement for more details.

Order now!

Reprints of this article can also be ordered at
http://www.dekker.com/servlet/product/DOI/101081SS100103628